Paper No. 250—8

Flow Characteristics around a Valve Plate Installed in a Duct*

(1st Report, Swing Type Valve Plate Installed at a Duct Exit)

By Junichi KUROKAWA**, Toshiyuki UCHIDA*** and Takashi KUSA****

The steady flow characteristics around a valve plate installed at the exit of a rectangular duct and the fluid force acting on the valve plate are studied experimentally, in order to determine the flow characteristics around flap valves, which are usually used to prevent reverse flow at the stop of pumping in large-size low-head pumps.

It is shown that the outlet flow has strong three-dimensionality with large lateral leakage from both sides of the valve plate, which results in that the outlet flow has the characteristics of a discontinuous separated flow rather than that of a jet flow. Empirical equations for pressure drop coefficient and moment coefficient around the plate axis are obtained, as well as a simple approximate method for estimating fluid force acting on the plate. The influence of an obstructing wall near the valve exit upon valve performances is also determined.

Key Words : Fluid Machine Element, Duct Flow, Flap Valve, Back Pressure, Drag Coefficient, Moment Coefficient

1. Introduction

The exit end of a discharge pipe of a large-size low-head pump is generally installed under the discharge water level, and a flap valve is used at the end of a discharge pipe in order to prevent a back flow from the upper water reservoir at the stop of pumping. In this case the opening of the valve plate changes largely with the change of the upper or the lower water level as the flow-rate changes largely with it. And in the range of large flow-rates the fluid force acting on the valve plate also becomes very large, which sometimes causes destruction of a stopper when the flap valve with a stopper is used. If the upper or the lower water level changes periodically, an oscillation is induced in the valve plate, which also induces destruction of the axis of the valve plate.

On the other hand, in a high-head pump a check valve is usually installed near the pump exit to prevent a back flow. Among the check valves usually manufactured a swing type is most popularly used, as its mechanism is very simple and the pressure loss in it is relatively small. But this type of valve plate can hardly follow a sudden change of flow-rate at the shut-off of the valve plate and a back flow is caused, or sometimes a self-excited vibration due to a sudden pressure change[1][2].

In order to prevent the above-described destructions of a flap valve, and to predict the response of a swing type check valve in a transient flow, it is first necessary to determine the steady flow characteristics, fluid force and energy loss. However, there are few studies about a steady flow characteristics around a flap valve[6] and a swing type check valve, though there are many about a transient characteristics for the combination of a swing-type check valve and a pump concerned in a water hammer phenomena[3]~[5].

This study is aimed at determining the steady flow characteristics around a valve plate, fluid force and loss of a flap valve installed at the end of a discharge pipe and a swing-type check valve installed midway in a pipe line near the pump exit. In the first report, the steady flow characteristics and fluid force of a flap valve installed at the discharge end of a rectangular duct are studied mainly by measurements.

2. Experimental Apparatus and Procedures

Experimental apparatus is shown in Fig.1. A rectangular duct of 300mm in height, 180mm in width and 1012mm in length is installed at the exit of a wind tunnel, and the valve plate of 338mm in length and 198mm in width is attached to the exit end of the duct with its upper end rotatably

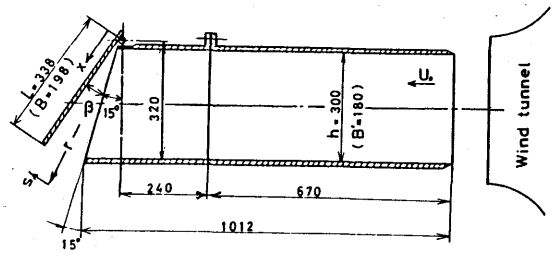

Fig. 1 Test stand.

* Received 2nd December, 1983.
** Associate Professor, Faculty of Engineering, Yokohama National University, (156 Tokiwadai Hodogaya-ku Yokohama)
*** Engineer, Torei Co. Ltd., (9-1 Ooecho Minato-ku Nagoya)
**** Engineer, Toshiba Co. Ltd. (1 Toshiba-cho Fuchu Tokyo)

supported. In a flap valve of practical use the exit end of a duct is usually cut diagonal as shown in Fig.1 in order to attain perfect shut-off performance and to shorten the shut-off time. The exit end of the present apparatus is also cut to 15 degrees.

In the first step of the experiment the flow characteristics in front of and behind the valve plate were measured by three-hole Pitot probes varying the valve opening angle β from 10 to 60 degrees and keeping the inlet velocity constant, and the static pressure distributions were measured along the valve plate and the duct wall. The moment around the valve plate axis was also measured by strain gauges attached to the axis. The measurements of the outlet flow were performed along the duct center at four sections, of which distances from the valve exit edge are 20, 40, 110 and 180mm (the radii ratio r/h are 1.20, 1.26, 1.49 and 1.73 respectively, where r is the distance from the valve plate axis and h is the duct height) by traversing the Pitot probe in the s-direction(see Fig.1) perpendicular to the main flow.

The influence of the obstructing wall installed behind the exit of the valve plate upon the valve performance is also determined experimentally for the purpose of practical applications.

3. Experimental Results and Discussions

3.1 Outlet flow from the valve plate

A transverse distribution of the outlet flow characteristics at 4 sections in the main stream direction is shown in Fig.2 for the case of the valve opening angle $\beta=22°$. The static pressure is not yet uniform at the section of 20mm (r/h=1.20) from the valve exit edge, but there exists a core-region where the total pressure is constant, which is similar to the two-dimensional jet. However, the decay of the core-region is very rapid and at 180mm from the valve exit edge (r/h=1.73) the core-region is not seen any more and the static pressure becomes uniform. In the case of a two-dimensional jet the distance of the decay of the core-region is known to be 5.4 times the jet width[7], but in the present case it is about 2.7 times the open width at the valve exit edge, which is about half of the two-dimensioinal jet.

Figure 2(b) shows that the outlet velocity profile just after the exit is relatively uniform, in spite of the anticipation that the velocity along the valve plate will be strongly accelerated and the velocity profile will be non-uniform at the exit due to a strong contraction of the channel and the non-symmetric exit profile. But a detailed examination of the velocity profile reveals that the vertical velocity component becomes larger in the upper half of the outlet flow and the horizontal one larger in the lower half.

The velocity profiles are compared in Fig.3 for various valve opening angles. The abscissa is the transverse distance s non-dimensionalized by the jet width w. The velocity distortion in the section becomes larger for smaller valve openings, but in the range of $\beta \geq 60°$ the vertical velocity becomes nearly zero and the distribution of horizontal ones becomes uniform. As such velocity distortion seems to contract the jet width and the entrainment of fluid from the outer periphery is hardly seen from Figs.2(b) and 3, the growth of the jet width is much smaller compared with the two-dimensional jet.

Figure 4 shows the distribution of the velocity vectors of the outlet flow for various valve openings. The direction of the outlet flow changes largely with β for a small value of β, but it becomes horizontal for large β. The jet width increases in the flow direction for small β, and becomes constant for $\beta=22°$, but for $\beta \geq 31°$ it decreases in the flow direction, which is quite different from the tendency of the two-dimensional jet.

The outlet flow characteristics, that is the jet width w, the section-averaged flow angle $\overline{\alpha_e}$ measured from the horizontal direction, the section-averaged velocity and the maximum velocity of the section, are plotted in Figs. 5 and 6 for the variation of the valve opening angle β.

Figure 5 shows that the mean outlet

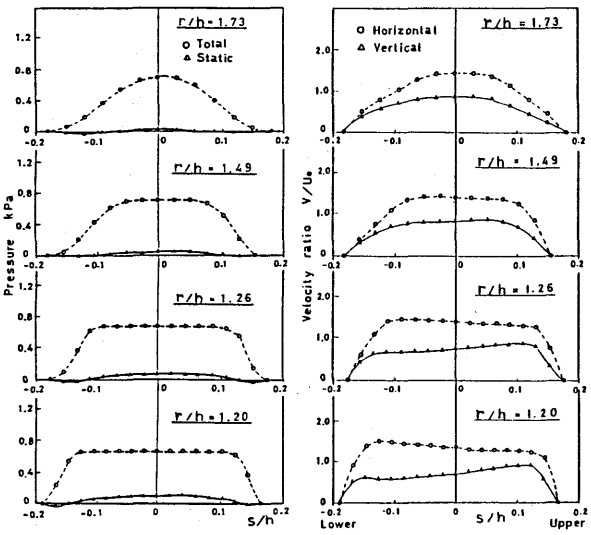

(a) Total and static pressure (b) Velocity
Fig. 2 Sectional distribution of outlet flow characteristics behind valve plate.

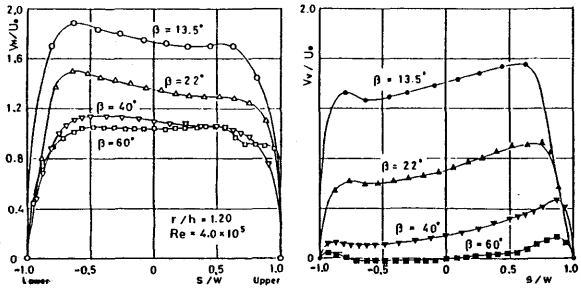

(a) Horizontal comp. (b) Vertical comp.
Fig. 3 Velocity distribution of outlet flow.

angle is nearly constant in the flow direction and decreases linearly with β, but comes close to zero in the range $\beta \geq 60°$. Also it shows that the jet width w increases linearly with β. For comparison the valve opening width w_0 is also plotted by a dotted line in the figure. It is of some interest that the contraction rate w/w_0 of the outlet flow at r/h=1.26 is 0.60 $\sim$0.65 and independent of β, which is equal to that of a discontinuous separated flow from a two-dimensional slit[9].

From Fig.6 the sectional mean velocity is seen to be nearly equal to the upstream velocity U_0 for $\beta \geq 30°$ in spite of the contraction effect of the channel, and in the range $\beta<30°$ it increases rapidly with a decrease in β. The maximum velocity of the section also shows the same tendency, but it changes little for the variation of the position r within the range tested, which suggests that there still remains the core-region at the centre of the jet.

In Figs. 5 and 6 the theoretical results by Birkhoff[8] are also plotted by a chain-dotted line. The theory by Birkhoff is aimed at analyzing the flow with a large cavity region formed at the back of a body set in a high velocity liquid flow, and the Hodograph-method is used under the assumption of a two-dimensional potential flow. They have given the solutions of the potential flow around the cavity region just behind the two-dimensional wedge shown in Fig.7. Dividing the flow field in two by the center line gives the present case. Figures 5 and 6 show that the theory gives good results only for the jet width w, and the other results are much larger than the measured ones. This is because the theory is based on the two-dimensional analysis and the real flow is largely influenced by the three-dimensinal lateral leakage due to the pressure difference between the front and the back side of a valva plate. Assuming that the leakage flow-rate is proportional to the square root of the differential pressure $\Delta p = p_0 - p_B$, where p_0 and p_B are the upstream and the back pressure respectively, the leakage flow-rate Q_L is given by

$$Q_L = CA'\sqrt{2\Delta p/\rho} \quad \cdots\cdots(1)$$

where $A' \fallingdotseq \beta L^2/2$ is the open space area of both sides of the valve plate and C is the flow-rate coefficient. The velocity reduction at the valve exit due to the leakage is then calculated as

$$\Delta V = 2Q_L/B'w \quad (B' : \text{duct width}) \quad \cdots\cdots(2)$$

Modifying the theory by V gives the dotted line in Fig.6 for the value of C=0.50, which is in good agreement with the measurements. This suggests that the lateral leakage has a significant influence upon the outlet flow of the flap valve. The difference between the chain-dotted line and the dotted line gives rough esti-

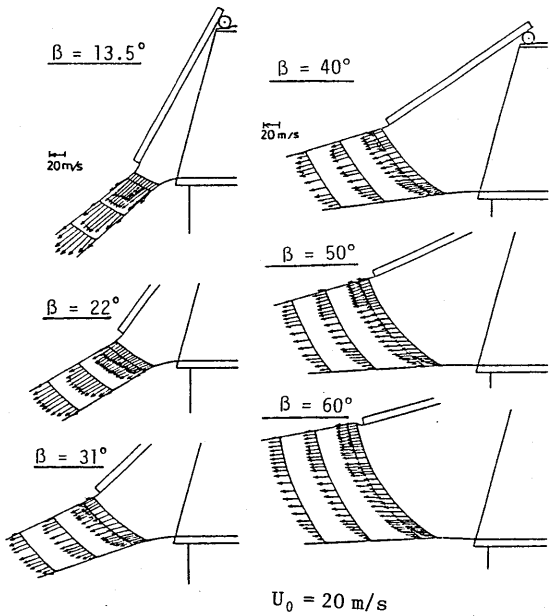

Fig. 4 Velocity diagram of outlet flow.

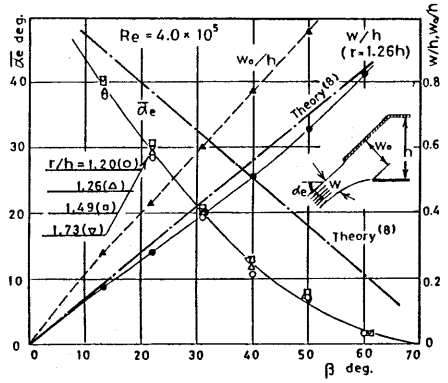

Fig. 5 Jet width w and section-averaged outlet flow angle $\overline{\alpha}_e$.

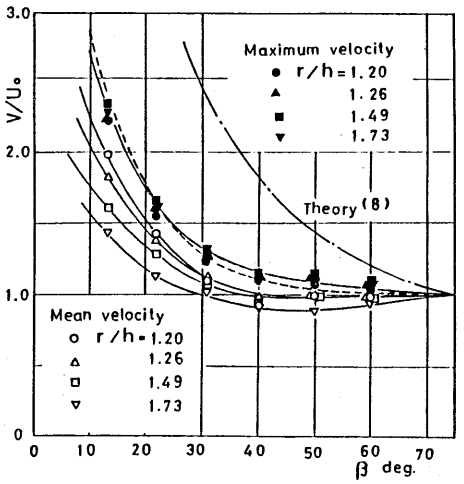

Fig. 6 Section-averaged velocity and the maximum velocity of the section.

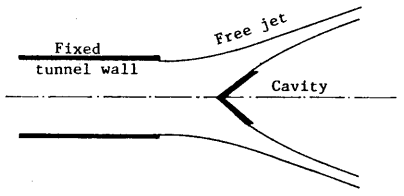

Fig. 7 Cavity flow model by Birkhoff et al.[8]

mation of the leakage flow-rate and the ratio of the leakage to the total flow-rate amounts to about 40 % at $\beta=40°$ and 60 % at $\beta=13°$.

After all, it is concluded that the differences of the valve outlet flow from the two-dimensional jet are based on the following reason: The valve outlet flow is under the dominating influence of the lateral leakage, while the two-dimensinal jet is based on the diffusion due to the fluid viscosity and the entrainment effect of the surrounding fluid. It then implies that the valve outlet flow is to be treated not as a two-dimensional jet flow into the same kind of fluid but as a separated discontinuous flow discharged into a different kind of fluid, such as a water flow discharged into atmosphere.

3.2 Pressure distribution on the valve plate and the fluid force

The pressure distribution on the valve plate is shown in Fig. 8 in the main-stream and transverse directions, and both the front and the back pressures are shown in the same figure, in which the pressure data are expressed as the difference from the upstream one p_0. It is shown that the pressures at the valve plate tip and both side edges drop considerably due to the influence of the back pressure and these low pressure zones become larger with a decrease in the valve opening angle, while in the other region the pressure decreases slightly and linearly toward the valve tip. It is also shown that the back pressure p_B decreases considerably with a decrease in β. Here it should be noted that the pressure over the front side of the valve plate except for the tip and both sides is expressed only as a function of the position and not of the valve opening angle. When calculating the fluid force acting on the valve plate by integrating the pressure distribution around the plate, good results might be expected by approximating $p=p_0$ over the whole length of the valve plate, because the negative pressure zone at the valve tip seems to be cancelled by the positive pressure zone in Fig.8(a). In the case of large β such approximation is not adequate but the fluid force becomes very small and raises no problem. However, in Figure 8(b) it is necessary to modify this approximation especially for the case of small β as the pressure drop at both side edges becomes larger with a decrease in β. As the profile of the non-dimensional differential pressure distribution $\Delta p/\Delta p_{max}$ is nearly the same for every valve opening angle as shown in Fig.9, the rate of the reduced fluid force due to the low pressure zone of both side edges is calculated to be about 22% (shown by the dotted lines in Fig.9). After all, rough estimation of the fluid force acting on the valve front side can be given by the following equation:

$$F=0.78A(p_0-p_B),\ A=BL \quad \cdots\cdots(3)$$

In Fig.8(a) some peculiar distributions are seen near the root of the valve plate. It is because this region is located in the separation zone just after the duct upper outlet edge.

As the lateral leakage has a dominating influence upon the flow characteristics around a valve plate, the theoretical results of the back pressure are much different from the measured ones, but the relation between the pressure along the valve plate and the outlet velocity must satisfy the similarity law, that is, the pressure divided by the dynamic pressure of the outlet flow must take the same value in both the theory and the measurements. Figure 10 shows comparison of the measured pressure coefficient with the theoretical one, and good agreement is seen.

One of the important performances of the flap valve is the pressure drop coefficient defined as

$$C_p=(p_0-p_B)\Big/\frac{\rho}{2}U_0^2 \quad \cdots\cdots(4)$$

The variation of Cp for the variation of the valve opening angle β is shown in Fig.11, from which the following empirical equation is obtained:

$$C_p=18.0\times10^{-0.0450\beta} \quad \cdots\cdots(5)$$

The loss coefficient of a flap valve is given by (Cp+1), as the total head of the outlet flow is discharged from the flap valve and is not recovered any more.

The pressure drop coefficient is a function of the Reynolds number $Re=U_0h/\nu$ as shown in Fig.12. It is well known that the drag coefficient of a body with sharp edge perpendicular to the flow direction becomes constant except in the low Reynold number

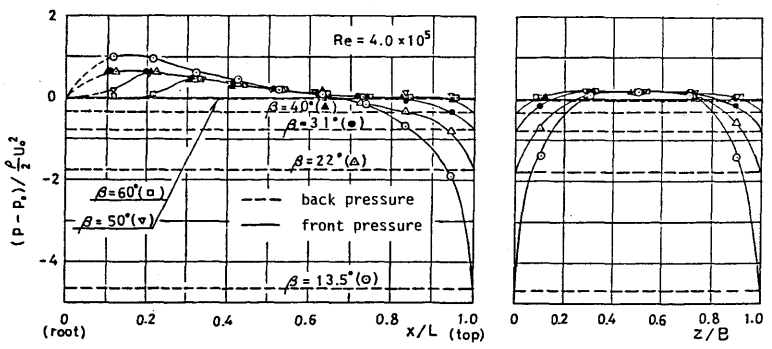

(a) In the mainstream derection. (z / B = 0.5)

(b) In the transverse direction.

Fig. 8 Pressure distribution and influence of valve openings.

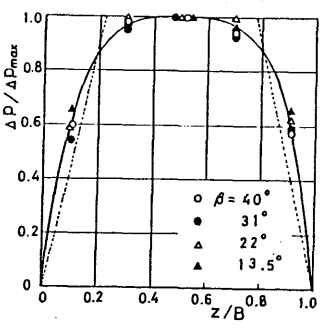

Fig. 9 Similarity of profile of transverse pressure.

range, as the separation point hardly changes with the variation of the Reynolds number. And in this case the pressure coefficient Cp was anticipated to take a constant value, but in Fig.12 the value Cp varies largely with Re in the case $\beta=13.5°$ and even in the case $\beta=22°$ it still decreases with Re. This might be because of the unstable separation point due to the finite thickness of the valve plate and also because of the reverse transition to the laminar flow due to a large negative pressure gradient as shown in Fig.8(a). However, flap valves are generally used in the large Reynolds number range, and it is considered that Equation (5) is valid for the practical application.

The fluid force F acting on the valve plate is given by integrating the pressure distribution around it, and the fluid force coefficient defined by

$$C_F=F\Big/\left(\frac{\rho}{2}U_0^2A\right),\quad A=BL \qquad \cdots\cdots(6)$$

is plotted against β in Fig.13. For comparison, also shown are the calculated results from various measured data, that is the measured moment data around the plate

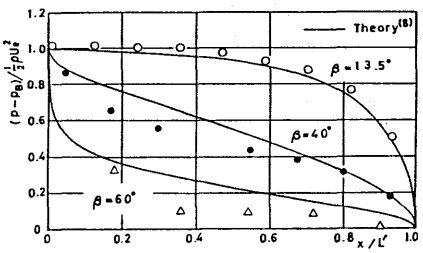

Fig. 10 Pressure coefficient defined as $(p-p_B)/(\rho Ue^2/2)$ and comparison with theory.

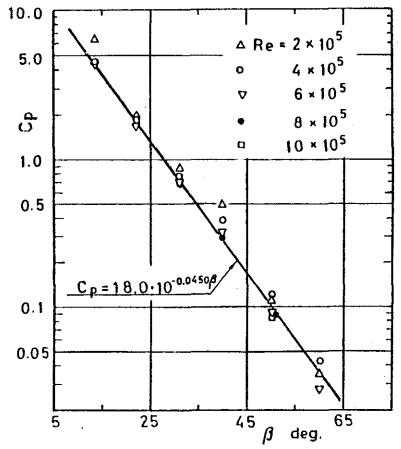

Fig. 11 Pressure drop coefficient.

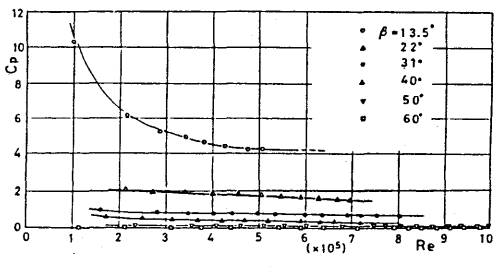

Fig. 12 Pressure drop coefficient vs. Re.

axis divided by the plate half length L/2 (marked O in the figure), the momentum change from the velocity data of the upstream and the downstream (Δ) and the results of Eq.(3) ($\bullet$). The non-dimensional form of the measured moment data is essentially to be called a moment coefficient:

$$C_M=M\Big/\left(\frac{\rho}{2}U_0^2\cdot A\cdot\frac{L}{2}\right) \qquad \cdots\cdots(7)$$

The result that the value of C_M agrees well with the value C_F means that the pressure distribution along the valve plate is nearly uniform, and the result that the value of $\bullet$ agrees well with the other ones means that a simple approximation of Eq.(3), or

$$C_F=0.78C_p \qquad \cdots\cdots(8)$$

is adequate for estimating the fluid force.

Lastly, the variation of the moment coefficient C_M is shown for the variation of the valve opening angle β in Fig.14, and of the Reynolds number Re in Fig.15. The tendency of the curves is similar to that of the pressure drop coefficient Cp in Fig.12, and the following empirical equation is obtained:

$$C_M=6.20\times10^{-0.0294\beta}\quad(\beta^\circ) \qquad \cdots\cdots(9)$$

Here for the case of $\beta=13.5°$ the value C_M has not yet become constant in the Re range tested as shown in Fig.14, but it is expected to be constant in the range of $Re>10^6$. The result calculated from the simple equation, $C_M\fallingdotseq C_F$, is also plotted in the figure by a dotted line, which gives somewhat different tendency from the measured results, and suggests that the approximate method of Eq.(3) is not adequate for estimating C_M values.

3.3 Influence of obstructing wall just behind the valve exit.

Flap valves are mounted at the duct outlet not only to the upper reservour of sufficient volume but also sometimes near the obstructing wall or into the midway of an open channel. In order to examine the influence of the obstructing wall in such cases, several kinds of obstructing walls shown in the right side of Fig.15 are set just behind the exit of the valve plate. The influence of the position of the obst-

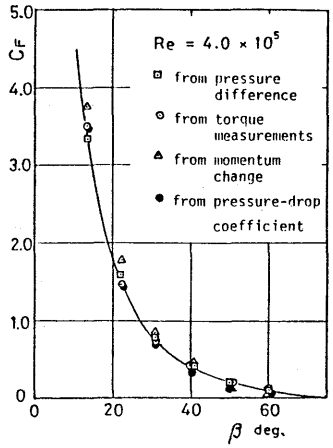

Fig. 13 Fluid force coefficient and comparison of various data.

ructing wall upon the moment coeffient is shown in Fig.15. It is seen that the influence of the obstructing wall becomes negligible when the obstructing wall is set more than twice the duct height apart from the duct exit for a large β and one time the duct height for a small β even if the L-type obstructing wall is set.

4. Conclusions

(1) The outlet flow from the valve plate has the characteristics of a separated discontinuous flow rather than that of a two-dimensional jet flow, as the lateral leakage from both sides of the valve plate has a dominating influence on the valve outlet flow characteristics. Within the range tested, the outlet flow width is contracted to 60 % of the valve open width and the maximum velocity of the outlet flow hardly changes in the flow direction. And the outlet flow angle is nearly proportional to the valve opening angle β in the range $\beta \leq 40°$, and in the range $\beta \geq 60°$ it becomes nearly zero.
(2) The pressure at the central part of the valve plate front side varies little for a wide variation of a valve opening angle due to large lateral leakage in spite of contracting effect of the channel. This leads to a simple approximate estimation of the fluid force, that is, assuming a constant upstream pressure over the whole front surface of the valve plate and calculating the 22% reduced force due to a pressure drop at both side edges.
(3) The empirical equations of pressure drop coefficient and moment coefficient are obtained in Eqs.(5) and (9). In the range of the Reynolds number of practical use these equations are valid.
(4) The similarity law is still valid between the outlet velocity and the pressure distribution along the center line of the valve plate, and the two-dimensional theory gives good results if the theory is adequately modified taking the leakage flowrate into account.
(5) The influence of the obstructing wall behind the valve exit is negligible when the valve is set more than twice the duct height apart from the wall in the case of large valve openings and one time the duct height in the case of small ones.

Acknowledgement

The authors would like to express their gratitude to Prof. R. Ooba, Tohoku University, for his valuable suggestions, to Dr. M. Ooshima and Mr. S. Saito, Ebara Co. Ltd., for the financial assistance of the experimental apparatus, and to Mr. J. Kawana for the assistance in the measurements.

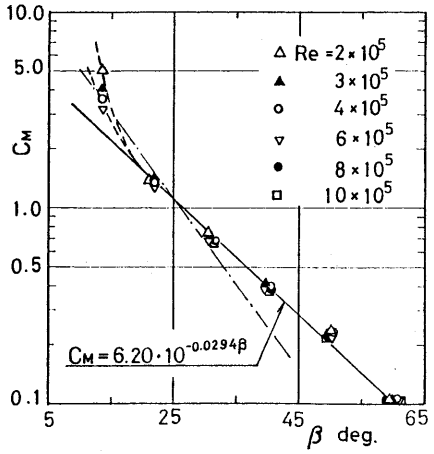

Fig. 14 Moment coefficient vs. β.

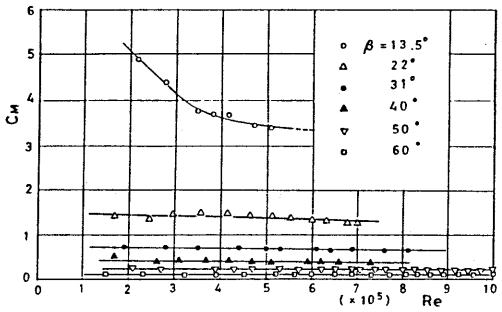

Fig. 15 Moment coefficient vs. Re.

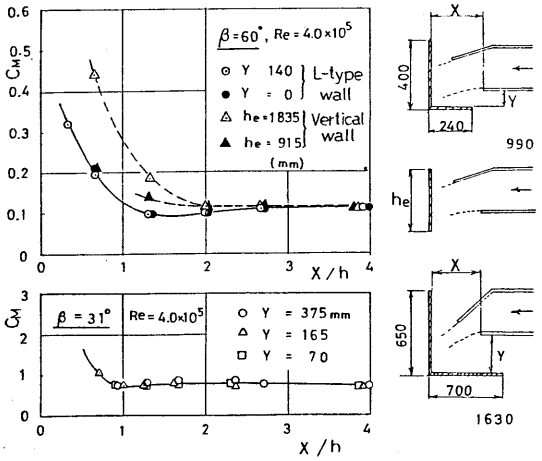

Fig. 16 Influence of obstructing wall behind valve exit on the moment coefficient.

References

(1) Weaver,D.S. and others, Trans. ASME, Ser.I, 100-3(1978), 239.
(2) Gwinn,J.M., ASME Paper, 74-PVP-51(1974).
(3) Teramae,H., Hitachi Hyoron(in Japanese), 33-5(1951), 35.
(4) Ikeo,S., Turbomachinery(in Japanese), 3-4(1975), 760.
(5) Yamamoto, K. and Nakamura, H., Turbomachinery(in Japanese), 9-10(1981), 579.
(6) Kane,R.S. and Cho,S.M., Proc. Am. Soc. Civ. Eng., HYI(1976), 57.
(7) Toyokura, T. and Kamemoto, K., Fluid Dynamics (in Japanese), (1981), 261, Jikkyo Shuppan.
(8) Birkhoff.G. and others, Quat. Appl. Math., 8-2(1950), 151.
(9) Imai, H., Fluid Dynamics, Part 1(in Japanese),(1974), 239, Shokabo.